# Performance Analysis of LoRa Radio for an Indoor IoT Applications

Eyuel D. Ayele, Chiel Hakkenberg*, Jan Pieter Meijers, Kyle Zhang, Nirvana Meratnia, Paul J.M. Havinga

Pervasive Systems Research Group, University of Twente, Enschede, the Netherlands
{e.d.ayele, j.p.meijers, k.zhang, n.meratnia, p.j.m.havinga}@utwente.nl

*c.hakkenberg@alumnus.utwente.nl

***Abstract*—LoRa is an emerging wireless standard specifically designed for Low Power Wide Area Networks (LPWANs). It provides long range, low data rate, and energy efficient wireless communication and is believed to have high potential for realization of a large number of Internet of Things (IoT) applications. Various research papers have already reported on the performance analysis of LoRaWAN protocol in terms of radio communication range, and reliability for outdoor environments, while performance analysis for indoor environments have not yet received enough attention. In this paper, we provide an in-depth performance evaluation of LoRa for indoor IoT applications.**

***Index Terms*—LPWAN, LoRa, LoRaWAN, Internet of Things, RSSI, performance analysis**

## I. Introduction

It is expected that by 2020 tens of billions of battery-powered data generating end-devices will be connected to the Internet [1]. The limited energy resource of these end-devices necessitates having low-power communication protocols in place. To this end, the low-power wide-area networks (LPWANs) have been designed to ensure a very long battery lifetime, specifically for applications requiring small amount of data to be transmitted over very long geographical distances. There exist various LPWAN-based technologies and solutions, such as UNB (Ultra Narrow Band) from Sigfox and WAVIoT Narrowband M2M protocol, and LoRaWAN [2]. Among all of them, LoRa (Long-Range) is believed to have high potential for realization of a large number of Internet of things (IoT) applications. While LoRa defines the physical layer of the communication link, LoRaWAN [1, 3] defines its open standard communication protocol. It enables a much larger range of machine-to-machine (M2M) and Internet of Things (IoT) applications as they are expected to tackle both the energy issue and infrastructure costs. By doing so, interconnecting a very large number of end-devices to each other and to the Internet, as envisioned by Internet of Things applications, seem to be feasible more than ever.

As part of LoRaWAN connectivity efforts, Semtech [4] released the LoRa RF platform (SX127X) that complements M2M cellular infrastructure and provides a cost-efficient way to connect battery operated mobile devices to the network infrastructure. LoRa physical layer protocol implements a spread-spectrum technique operational in the sub-GHz frequency spectrum such as 433MHz, 868MHz, and 915MHz, which have less interference with other frequency bands such as 2.4GHz used by WiFi and Bluetooth [3]. In principle in these sub-GHz bands, signals are more robust against noise while drawing relatively low energy. This makes them ideal for many IoT applications.

978-1-5386-2064-9/17/$31.00 

Since the release of the first version of the LoRaWAN specification by the LoRa Alliance [3], some research papers reported on the performance analysis of LoRaWAN protocol in terms of radio communication range, and reliability. For instance, Wendt et. al [5] presented their analysis of LoRa radio's signal wall penetration in an indoor environment by observing the RSSI values. The capacity and scalability of LoRaWAN were studied by [6, 7]. In [8], the authors have evaluated LoRa's communication range and developed an outdoor propagation model. They stated to have reached a communication range of 15 km in air. They also developed a channel attenuation model for estimating the communication distance between LoRa end-devices and LoRa gateways. Brecht et. al [9] compared LoRaWAN with other long-range unlicensed technologies in terms of communication range and coexistence capabilities. They also analyzed the long-range performance in terms of packet error rate and throughput without explicitly analyzing the propagation characteristics.

Complementary to research of LoRa performance evaluation for outdoor IoT applications, in this paper we focus on indoor IoT applications. To this end, the contributions of this paper include: (1) testing the decoding performance of LoRa radio receivers and comparing it with the specification defined by the LoRa Alliance [3]; (2) performance analysis of LoRa in terms of link quality between the LoRa end-devices and the gateway, looking specifically into packet loss and received signal strength (RSS); (3) proposing a suitable LoRa radio configuration including the LoRa radio spreading factor to improve performance for indoor environments.

The rest of this paper is organized as follows. LoRa protocol specification and its network architecture are introduced in Section II. The indoor experimental set-up and discussion of test results are presented in Section IV, followed by concluding remarks in V.

## II. Specification of LoRaWAN protocol and network architecture

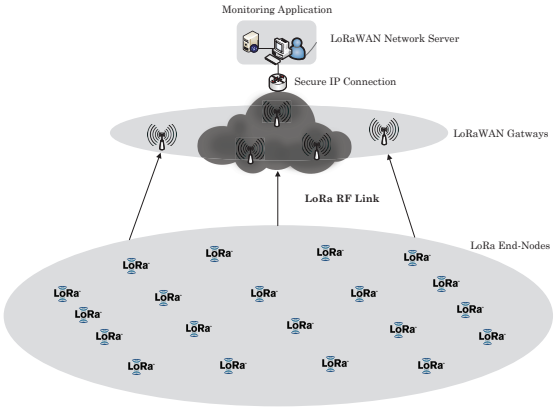


*Fig. 1: Generic LoRaWAN Star Network Topology Architecture*

LoRa radio link is based on a proprietary chirp spread spectrum modulation scheme. LoRaWAN is the medium access control protocol of the LoRa standard. Relative to the OSI reference model, LoRa represents the physical layer (layer 1) while LoRaWAN represents layer 2 and layer 3. Figure 1 shows the network architecture for setting-up a LoRaWAN infrastructure. The LoRaWAN communication is achieved through a simple star topology. The network architecture includes three components, i.e. end-devices, gateways, and a network server. LoRa gateways forward the control signals and the generated data messages of the end-devices to a central network server and are able to decode multiple signals at the same time. The LoRaWAN specification [3] defines that the LoRa gateways are connected to the network server with an IP connectionn and the end-devices communicate to the gateway through a single hop wireless communication. Communication between LoRa end-devices and LoRa gateways is bidirectional to support services such as software upgrade, over-the-air activation, and multi-casting. The network server is used as the sole manager of the network. It can manage, among other things, the communication data rate settings for each end-device separately through the adaptive data rate (ADR) scheme.

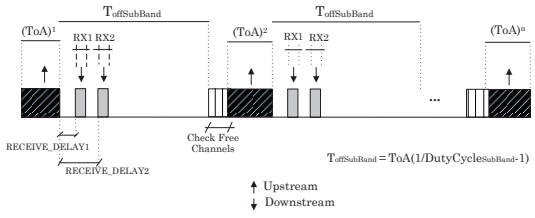


*Fig. 2: LoRa channel access for Class-A end-devices, where $ToA$ is the data frame Time-On-Air and $T_{offsubBand}$ is the off channel time in seconds.*

The LoRaWAN specification [3] describes three classes of end-devices (i.e. Class A, Class B, and Class C). The difference between these classes relates to the timing of the so-called receive-window. Class A is the default LoRa end-device operation as shown in Figure 2. It allows a bidirectional link with the gateway, whereby each end-device's upstream transmission is followed by two time-slots for a short downstream reception. Class B end-devices allow a bi-directional link with scheduled listening time-slots, whereas Class C end-devices allow continuous listening time-slot but the listening slot will be closed during transmission.

Depending on the data rate used, it takes a certain amount of time to complete an upstream data transmission. This time is called $Time-On-Air$ ($ToA$) (see Figure 2). After $ToA$ has passed and due to the ETSI imposed restrictive of 1% transmission duty-cycle per sub-band ($DutyCycle_{subBand}$) [10], the end-device is not allowed to access the channel for at least $T_{offsubBand} = ToA \times (1/(1 - DutyCycle_{subBand}))$ seconds.

The $ToA$ is expressed by Equation 1, where $n_{preamble}$ is the number of preamble symbols $n_{preamble}$=8, $PL$ is the number of $PHY$ payload bytes, and $CRC$ and $H$ specify the presence of $CRC$ and $PHY$ header, respectively.

$$ToA(PL) = (T_s) \times \left( (T_{pre}) + max\left\{ \lceil \Gamma \rceil \times (CR + 4), 0 \right\} \right) \quad (1)$$

where the symbol period $T_s = (2^{SF}/BW)$, the preamble length $T_{pre} = (n_{preamble} + 12.25)$, $\Gamma = \left[ \frac{8PL - 4SF + 28 + 16CRC - 20H}{4 \times (SF - 2DE)} \right]$.

LoRaWAN specification [3] prescribes $CRC = 1$, $H = 0$ for uplink, $CRC = 0$ and $H = 0$ for downlink. The Low Data Rate Optimization feature (denoted by DE) is a feature that aims to improve the robustness of the transmission to frequency variations during the transmission of the packet on high spreading factors ($SFs$) which is obligatory for low bit rate settings. $CR$ indicates coding rate ranging between 1 and 4 where $CR = 1$ corresponds to a $4/5$ coding rate and $CR = 4$ corresponds to the maximum coding rate of $4/8$.

As shown in Figure 2, for every successful transmission, an end-device will have two receive windows, during which it can receive downstream messages. The first receive window uses the same frequency channel as the preceding upstream message and a data rate that is a function of the data rate used for the preceding upstream message. By default, the data rate of the first receive window is identical to the data rate of the last upstream. $RX1$ opens $RECEIVE\_DELAY1$ seconds after the end of the upstream modulation. The second receive window uses a configurable, non-adaptive, channel and data rate and opens $RECEIVE\_DELAY2$ (=$RECEIVE\_DELAY1$ +1s) seconds after the end of the upstream modulation. The frequency and bit rate used can be modified by the LoRaWAN MAC commands. The LoRaWAN

channel access scheme is similar to the Aloha MAC [3], in which LoRa end-devices could access the channel randomly.

## III. LoRa Physical Layer Parameters and Their Expected Impact

When testing the performance of LoRa, it is critical to measure a variety of physical layer parameters that impact the performance of the radio link. The three physical layer parameters, namely, Spreading factor (SF), Bandwidth (BW),and Coding Rate (CR), influence the effective bit rate of the modulation, its resistance to noise and interference, and its ease of decoding.

| BW \ SF | 7 | 8 | 9 | 10 | 11 | 12 |
|---|---|---|---|---|---|---|
| 125kHz | -123 | -126 | -129 | -132 | -133 | -136 |
| 250kHz | -120 | -123 | -125 | -128 | -130 | -133 |
| 500kHz | -116 | -119 | -122 | -125 | -128 | -130 |

*TABLE I: Semtech LoRa receiver sensitivity specification in dBm for various BW and SF settings (data sheet [3]). SF = Spreading Factor, BW = Band Width.*

Table I shows a summary of the expected receiver sensitivity with respect to BW and SF, using LoRa radios sd reported in the SX1276 data sheet [3]. We aim to compare our test results with this specified sensitivity values to evaluate how the practical implementation deviates from the expected values. LoRa radio channel bandwidth determines the noise floor and thereby the receiver sensitivity. It is expected that an increase in channel bandwidth results in decrease of the receiver sensitivity, and the higher spreading factor the higher the receiver's sensitivity. Furthermore, an increase in coding rate improves the packet delivery ratio.

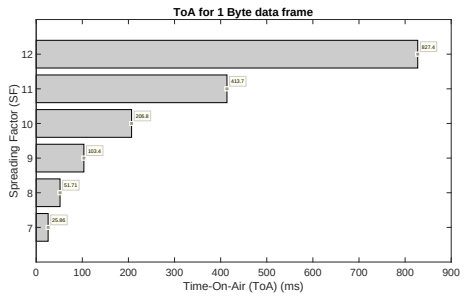


*Fig. 3: Time-on-air (ToA) (frame duration) for various spreading factor (SF) settings. For higher SF results in higher ToA*

Theoritically, the expected impact of the four LoRa physical layer parameters can be summarized as follows:

***Spreading Factor (SF):*** A high SF should be easily decodable, resulting in a high $Time{-}on{-}Air$ (Figure 3), lower PER and lower minimum RSSI. A lower SF therefore should result in a higher PER and a higher minimum RSSI.

***Coding Rate (CR):*** A higher CR transmits more redundant data bits, consequently producing a lower overall PER.

***Transmission Power (TXP):*** A high TXP will result in a higher RSSI, increasing the range of reception while allowing a lower PER.

***Band Width (BW):*** A smaller BW increases the receiver sensitivity while lowering the noise floor, allowing a lower PER.

We perform measurements on all spreading factors supported by the LoRa end-device at 868MHz frequency band and 125KHz bandwidth, as presented in Table II for LoRa radio parameter settings. The transmit power (TXP) is fixed at the maximum value of 14dBm for LoRaWAN end-devices for the EU868MHz band, unless explicitly defined differently. For the bandwidth (BW) we use the default LoRaWAN value for the EU868MHz band, which is 125KHz. In theory, the useful bit rate is $R_b = SF \times (BW/2^{SF}) \times CR$, which shows that a higher bit rate can be achieved with a broader bandwidth. This is however not possible on the default EU868Mhz LoRaWAN channels.

## IV. Performance Evaluation of LoRa Radio in an Indoor Environment

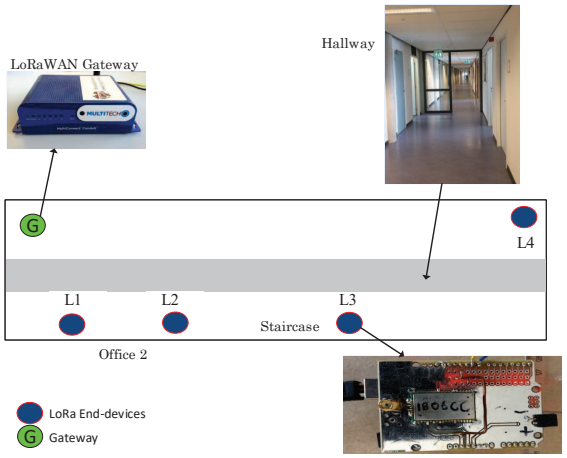


*Fig. 4: LoRa End-nodes deployment across building hallway floor at locations L1 to L4. The four locations are chosen in an increasing order of transmission range from the gate way, which is located at the left corner of the building.*

To evaluate performance of the LoRaWAN protocol in an indoor environment, we built a LoRa radio enabled end-device using *RN2483* and Arduino Uno modules and mounted the LoRa radio module on top of a custom made Arduino shield equipped with an antenna. The prototyped end-device is shown in Figure 4.

The receiving node of the network (the LoRa gateway) is a *MultiConnect Conduit MTCDT-H5-210L* gateway, as shown in Figure 4, manufactured by MultiTech [11]. Since the gateway is designed to listen for incoming messages on the 868MHz band, all end-devices support the three default channels (0, 1 and 2, i.e. 868.1, 868.3, 868.5 MHz) that must be implemented in every EU868MHz end-device to comply

with the LoRaWAN specifications. We set up a local *Node.js* web application as the server-side of the LoRa network server. It runs a *Mariadb* database to collect and store the transmitted packets from the LoRa end-devices. The database provides various information about the received packets such as RSSI values and sequence number.

### A. Deplyment

Figure 4 shows the LoRa gateway deployment at one of the buildings of the *University of Twente* campus, where our experiments took place. The indoor experiments were performed with end-devices and a gateway placed on one floor of our office building as shown in Figure 4, the floor is roughly 103m by 20m. To test LoRa for different communication scenarios, the transmitting end-devices were placed at four locations (denoted by L1 - L4 in Figure 4) on the floor while the receiving gateway was placed at the corner of the building. Experiments were performed during normal office working hours to include the influence of people movements and environmental dynamics on LoRa network performance.

As mentioned in Section II, due to the channel access restrictions imposed on EU863-870MHz LoRa operating frequency, data packets will defer their next data packet transmission for a time period of at-least $T_{OffSubBand}$. Changing the spreading factor (SF) results in a change in $T_{OffSubBand}$ and time on air $ToA$, which will subsequently result in a change in the link budget, i.e. battery lifetime versus range trade-off. For example from Equation 1, it will take at least 3.8 hours for $SF = 12$ and 21 minutes for $SF = 7$ to finish sending a 50 Byte long data frame. This is in accordance with the 1% duty-cycle regulation, calculated with respect to the payload size for every spreading factor settings. In addition all the measurements are performed using unconfirmed mode (unacknowledged) data frame types to prevent the acknowledgement from clogging the channel for upstream packets.

### B. Impact of Received Signal Strength Indication (RSSI)

To test the overall capability of LoRa radio receiver to demodulate data from a received signal, we analyze the received packets in terms of their RSSI values. These values are compared to the Semtech SX1276 LoRa receiver theoretical sensitivity which is specified for various BWs and SFs [4] settings (Table I). In our experiment the end-device transmits 50 data packets, each with 50 bytes of payload, at every test location, and for every SF. All packets are unconfirmed with no retransmissions, as presented in Table II.

Figure 5 shows the minimum RSSI measured at locations L1, L2, L3, and L4. As the number of obstructions (non-line-of-sight) and distance to the gateway increases, the RSSI values decreases. This trend is observed for all SF values. Theoretically as explained in III, one would expect the minimum RSSI for received packets decrease as the SF value increase. In our results this is only true for SF7, SF10, SF11, and SF12. In case of SF8 and SF9, SF9 performs better than expected, and SF8 performs *even much* better. In other words, SF7 and SF8 are performing as expected, while SF9 up to SF12 perform worse than expected. It is not possible to prove this by only looking at the RSSI. Therefore we also measure the packet error rate and analyze it in the next section. A possible alternative reason for the unexpected high minimum RSSI values for higher SFs is the way the RSSI is calculated. For higher SFs, a packet has a longer $Time - on - Air$ (Equation 1), giving a longer time over which the signal strength can be integrated. This depends on the method implemented inside the proprietary ("black box") LoRa radio module.

For locations closer to the gateway, the link fluctuation is high for high SFs, with maximum standard deviation of $\sigma = 4.18dBm$. The link is observed to be more stable at the farthest location at high SFs (SF11, SF12), with maximum change of $\sigma = 3.6dBm$ only.

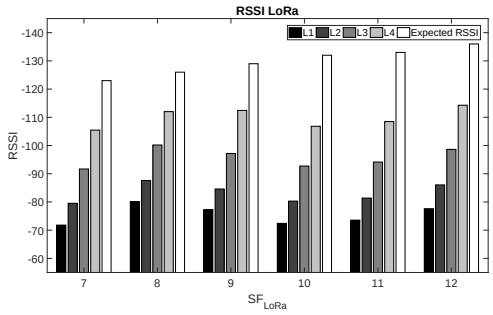


*Fig. 5: Minimum RSSI (in dBm) for SF=7 to 12 at locations (L1, L2, L3 and L4).*

### C. Impact of Packet Error Rate (PER)

Figure 6 illustrates the packet error rate (PER) versus LoRa end-node locations (L1-L4) for spreading factors SF7 to SF12. The transmitted LoRa packet is set to unconfirmed with no retransmission. End-devices transmit 50 data packets each with 50 bytes of payload for every test location. One can see that in general the packet loss has an increasing trend when the transmitter end-device is farther from the gateway location. From the theoretical analysis presented in Section III, we expect that a higher SF should result in a lower PER. This is, however, not observed at any one of the four locations.

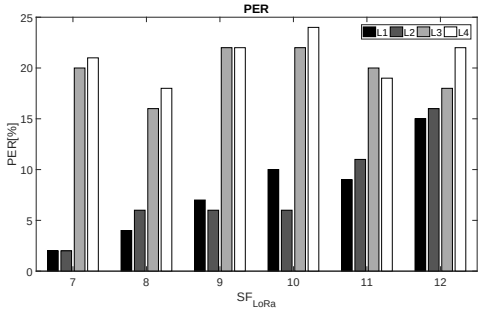


*Fig. 6: Packet Error Rate (PER) for SF=7 to 12 at Locations (L1, L2, L3 and L4).*

| LoRa settings | | |
|---|---|---|
| **Parameter** | **Value** | **Details** |
| Center Freq. | EU 868MHz | Class A (Either of the Default three channels in case of 868MHz band) |
| Band Width (BW) | 125Hz | Default for LoRaWAN configuration |
| Spreading Factor (SF) | SF7-SF12 | SF7-SF12 are to be set (as per [3]) |
| Tx-Power | 14dBm | The maximum default tx power for 868 MHz |
| Tx Payload Size (byte) | 50 | (used with all Spreading Factors (SF) |
| Data Frame Mode | Unconfirmed | Unacknowledged data frame |
| **Radio Antenna Properties** | | |
| End-Mote | Frequency range: 868MHz, Gain: 2.1dBi | RN2483 MICROCHIP LoRa Module, VSWR: $< 1.5$ |
| Gateway | Female SMA, 2dBi | Detachable Omni-directional antennas MUTITECH-Gateway |

*TABLE II: LoRa Radio parameter settings used in the performance test.*

Since the LoRa gateway is placed in an indoor environment, it is more susceptible to indoor signal shadowing and multi-path fading. Using high spreading factors, such as SF=12, increases the $Time - on - Air$ as expressed by Equation 1, resulting in a 50 byte payload LoRaWAN packet to have a $ToA = 2794$s. In an indoor environment with people moving around signal paths can change very fast.

The reason for higher SFs to perform worse than lower SFs is partly related to the longer $ToA$ of higher SFs. When a packet is received by the gateway, the preamble of the packet is used by the receiver to lock onto the transmitter. This "*locking on to*" means both synchronizing in time and adjusting the gain of the receiver's preamplifier. Preamplifiers can have a relatively small dynamic range compared to the variations in the signal path at an indoor location. Our theory is that a packet with a long $ToA$ will be received at a specific preamplifier setting, but shortly after this the signal strength will change rapidly because of multiple signal paths as well as quick fading due to movement of people in the building. As soon as the received signal strength falls outside the dynamic range of the receiver's preamplifier, the rest of, or part of the packet is not received. For longer packets, the fraction of the packet that is not received becomes more significant, causing the forward error correction to fail. For lower SFs, the $ToA$ is much shorter. This lowers down the chance of falling outside the dynamic range of the receiver. This will lower down the fraction of the packet that is not received and will consequently increase the probability of the forward error correction to succeed.

If our assumption about the preamplifier in the *"black box"* proprietary LoRa receiver is correct, then the results illustrated in Figure 6 can be described as follows: closer to the gateway, packets with shorter $ToA$s are more likely to be received. For locations further from the gateway, lower spreading factors are more likely to fail. Location L1 is close to the gateway and the effect of packet ToA can be clearly seen. The further we go from the gateway, the effect of SF is more visible as PER is rapidly increased for lower SFs and slightly increased for higher SFs.

### D. Impact of Coding Rate (CR) and Transmission Power

The idea behind this set of experiments is to evaluate the impact of the Coding Rate and the transmission power on LoRa performance by fixing the Data Rate. To do so, instead of transmitting at different spreading factors, all packets are sent at a fixed SF.

In the first experiment, we transmit 15 packets on each coding rate, transmission power and three data rates, i.e., DR 5, DR 3 and DR 1 at each transmission round. After every 15 packets, the coding rate is increased until the maximum is reached. Then the coding rate is set back to the minimum and the transmission power is decreased by one. The end-devices were programmed to start at DR5, coding rate 4/5, and transmission power of 14 dBm. After each 15 packets, the coding rate was increased until the maximum of 4/8 was reached. Then the transmission power was lowered one step and the same process was repeated. The packet loss from the end-device at location L3 transmitting on DR5 (i.e. SF=7) is shown in Figure 7. It can be seen that generally transmitting packets with a higher transmission power decreases the packet loss.

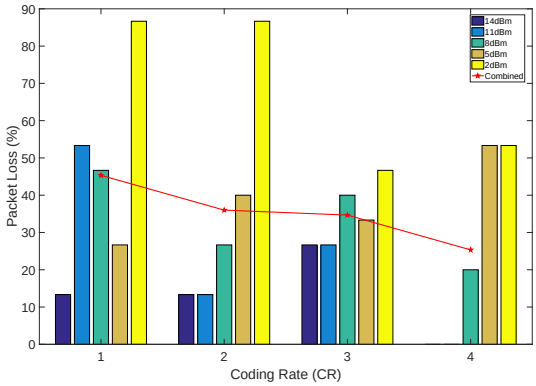


*Fig. 7: The packet loss from the end-device at location L3, transmitting on DR=5; for varying transmission power and coding rate.*

We repeat the same experiment with DR3 and DR1. Figures 8 and 9 show the results. One can see that When the data rate is decreased (resulting in an increase of the spreading

factor), the packet loss decreases as well. This behavior is expected from the spread spectrum concept as signals with higher spreading factors are more likely to reach a gateway. There are, however, also some notable differences in packet loss between the end-device at different CRs.

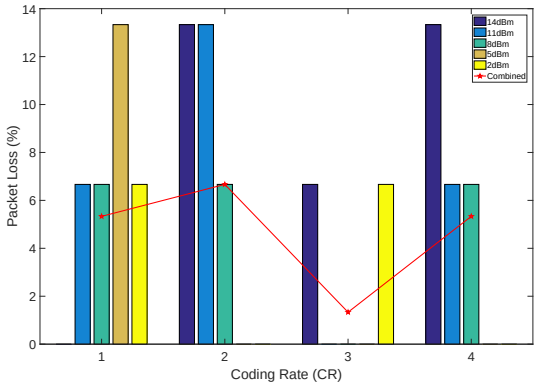


*Fig. 8: The packet loss from the end-device at location L3, transmitting on DR=3; for varying transmission power and coding rate.*

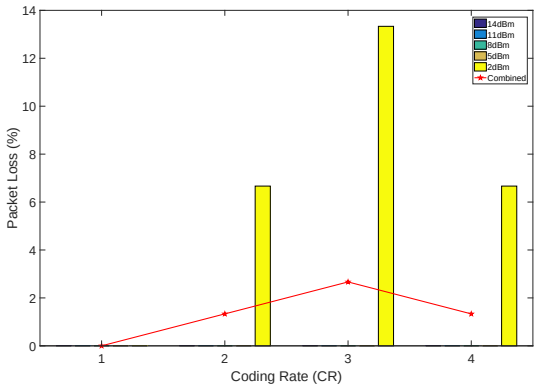


*Fig. 9: The packet loss from the end-device at location L3, transmitting on DR=1; for varying transmission power and coding rate.*

Some end-devices show a slightly higher packet loss at higher coding rates or transmission powers, which contradicts the expected lower packet loss at higher coding rate and transmission powers. The numerical differences between the lost packets on different transmission settings are, however, small and might have been caused by environmental changes of office environment due to factors such as people moving around and doors being opened and closed.

## V. Conclusion

In this paper we studied LoRa wireless technology, a new LPWAN protocol for IoT applications, and conducted its network performance analysis. A general overview of LoRa modulation and network architecture is introduced. The associated LoRa physical layer parameters such as spreading factor, bit rate and coding rate are discussed. We built and prototyped LoRa radio enabled network, to test the network performance From our investigation of LoRa radio RSSI values, we observed that due to the broadband chirp pulses and higher sensitivity of the LoRa modulation, LoRa offers immunity against multi-path and signal fading especially at high spreading factor. At closer distances to the gateway, the RSS is high for low spreading factor scheme. In addition to that, when the spreading factor is increased the packet loss decreases at the expense of decreased effective bit rate, which is not suitable for high throughput IoT applications. And at farthest locations from the gateway interferences are significantly high, therefore, end-devices should communicate at high spreading factors.

## Acknowledgment

This research was supported by the Smart Parks Project, funded by the Netherlands Organization for Scientific Research (NWO).

## References

[1] A. Mohammed Al-Fuqaha, A. Guizani and A. Moussa. Internet of things: A survey on enabling technologies, protocols, and applications. *IEEE Communications Surveys Tutorials*, 17(4):2347–2376, 2015.

[2] M. Centenaro, L. Vangelista, A. Zanella, and M. Zorzi. Long-range communications in unlicensed bands: The rising stars in the iot and smart city scenarios. *IEEE Wireless Communications*, 23(5):60–67, 2016.

[3] Lora alliance–wide area networks for iot. *[Online]. Available: https://www. lora-alliance. org/[Accessed: 06 February 2016]*, 2016.

[4] Sx1276, August 2016. [online] http://www.semtech.com/wireless-rf/rf-transceivers/sx1276/.

[5] T. Wendt, F. Volk, and E. Mackensen. A benchmark survey of long range (loratm) spread-spectrum-communication at 2.45 ghz for safety applications. In *WAMICON, 2015 IEEE 16th Annual*, pages 1–4. IEEE, 2015.

[6] K. Mikhaylov, J. Petäjäjärvi, and T. Haenninen. Analysis of capacity and scalability of the lpwan technology. In *22th EWC; Proceedings of*, pages 1–6, 2016.

[7] A. Augustin, J. Yi, T. Clausen, and W. Townsley. A study of lora: Long range & low power networks for the iot. *MDPI Sensors*, 16(9):1466, 2016.

[8] J. Petajajarvi, K. Mikhaylov, A. Roivainen, T. Hanninen, and M. Pettissalo. On the coverage of lpwans: range evaluation and channel attenuation model for lora technology. In *ITS, 2015 14th Conf. on*, pages 55–59. IEEE, 2015.

[9] B. Reynders, W. Meert, and S. Pollin. Range and coexistence analysis of long range unlicensed communication. In *ICT, 2016 23rd International Conference on*, pages 1–6. IEEE, 2016.

[10] TR ETSI. Tr 102-313 v1. 1.1,". *ERM, pp8*.

[11] Multitech, Aug. 2016. [online] http://www.multitech.com/.